Pharmacogn. Mag.
A multifaceted peer reviewed journal in the field of Pharmacognosy and Natural Products
www.phcog.com | www.phcog.net

ORIGINAL ARTICLE

Comparative *in vitro* and *in silico* Characterization of anticancer Compounds Piceatannol, Biochanin-A and Resveratrol on Breast Cancer Cells

Pardhasaradhi Mathi[1], Neelima Musunuru[2], Udayapriya Adurthi[2], Mahendran Botlagunta[2,3]

[1]Department of Biotechnology, Upstream Process Development, Sun Pharmaceutical Industries, Ltd, Vadodara, Gujarat, [2]Department of Biotechnology, Koneru Lakshmaiah Educational Foundation (K L [Deemed to be University]), Guntur, Andhra Pradesh, [3]Department of Indo American Cancer Research Foundation, Basavatharakam Indo-American Cancer Hospital and Research Institute, Banjara Hills, Hyderabad, Telangana, India

Submitted: 01-04-2019 Revised: 13-05-2019 Published: 28-11-2019

ABSTRACT

Background: Biochanin-A and Piceatannol are phytochemical constituents extracted from *Sophora interrupta*. Although both the compounds were isolated from a single plant, these compounds were not compared against anticancer activity. **Objective:** A systematic comparative analysis of biochanin-A, piceatannol, and resveratrol was performed to investigate cancer cell viability, motility, metabolic changes in Michigan Cancer Foundation-7 breast cancer cells, and structure compound interaction with the vascular endothelial growth factor (VEGF) receptors were studied. **Materials and Methods:** Cancer cell viability was studied using 3 (4, 5 dimethyl thiazol 2yl) 2, 5 diphenyltetrazo- lium bromide and acridine orange (AO)/ethidium bromide (EtBr) assay. The wound-healing assay was performed by measuring cell migration from the scratch area. Metabolic changes of the compounds in culture conditions were recorded using Fourier-transform infrared (FT-IR) spectroscopy. Molecular docking and dynamic simulations were performed using Schrödinger software. **Results:** Our results showed that the half-maximal growth inhibitory concentration for biochanin-A is 150 μM/ml and piceatannol and resveratrol showed 150 μM/ml, which is evident from the uptake of AO and EtBr dyes by live/dead cells. Moreover, drug-treated cells were unable to fill the cleared area from the scratch area, which suggests that all compounds effectively inhibit cell motility. FT-IR fingerprint showed a marked difference in the percentage of transition and dynamic structural changes between untreated and treated samples. Strong hydrogen-bond interaction with VEGF receptor-1 (VEGFR1) and VEGFR2 proteins and their interactions were stable throughout the simulation period. Moreover, these compounds inhibited sprouting of a new blood vessel from the chicken aorta and microvessels formation in the *in ovo* chorioallantoic membrane assay. **Conclusion:** Taken together, we conclude that anticancer and anti-angiogenic activity, structure-function relationship of biochanin-A is like well-known anticancer compound resveratrol and its metabolic product piceatannol in breast cancer cells.

Key words: Biochanin A, cancer cell viability, chorioallantoic membrane assay, molecular dynamic simulations, molecular docking, piceatannol, resveratrol

SUMMARY

- The study investigates the comparative *in vitro* and *in silico* characterization of piceatannol, biochanin-A, and their structure-function relationship with a well-known anticancer compound resveratrol. Results showed that the inhibitory concentration values for biochanin-A is lesser than resveratrol and its metabolic product piceatannol in Michigan Cancer Foundation-7 breast cancer cells and these compounds effectively blocked the cell migration, which is evident from the *in vitro* scratch assay. Fourier-transform infrared analysis confirms the uptake of compounds by Michigan Cancer Foundation-7 cells, which is evident from a marked difference in the percentage of transition in the media, in the cells as compared to compound alone. Molecular docking and molecular dynamic simulation analysis showed that all three compounds form a strong hydrogen-bond interaction with a well-known angiogenic factor such as vascular endothelial growth factors receptor 1 and vascular endothelial growth factors receptor 2 throughout the simulation period (10 ns), and their anti-angiogenic activity was further confirmed by validating sprouting of the new blood vessel from the chicken aorta. Taken together, we conclude that biochanin-A data are in accordance with a well-known anticancer compound resveratrol, and further studies are required to know the comparative molecular mechanism toward an anticancer activity.

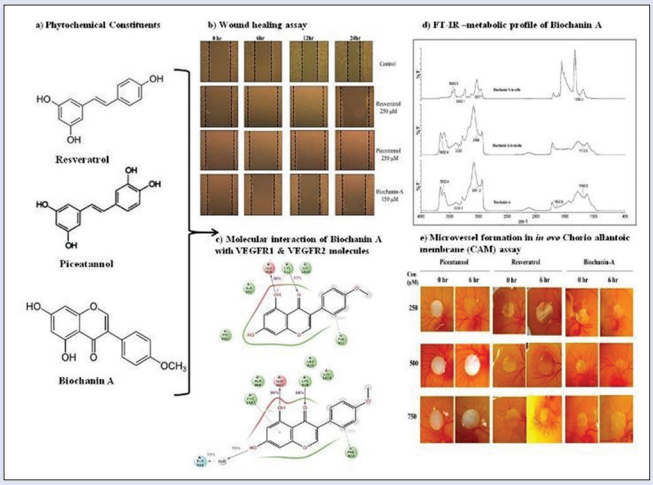

Abbreviations used: VEGF: Vascular endothelial growth factors; TRAIL: Tumor necrosis factor-related inducing ligand; MCF7 Cells: Michigan Cancer Foundation-7; CAM: Chorioallantoic membrane; DMEM: Dulbecco's modified Eagle's medium.

Correspondence:

Dr. Mahendran Botlagunta,
Department of Biotechnology, Koneru Lakshmaiah Educational Foundation (K L [Deemed to be University]), Guntur, Andhra Pradesh - 522 502, India.
E-mail: bmnchowdary@gmail.com

DOI: 10.4103/pm.pm_146_19

Access this article online
Website: www.phcog.com
Quick Response Code:

Cite this article as: Mathi P, Musunuru N, Adurthi U, Botlagunta M. Comparative *in vitro* and *in silico* characterization of anticancer compounds piceatannol, biochanin-A and resveratrol on breast cancer cells. Phcog Mag 2019;15:S410-8.

INTRODUCTION

Biochanin A is one of the dietary constituents found in soy, peanut, and chick pea.[1] In *in vivo*, this compound can be metabolized to genistein (angiogenesis inhibitor).[2] Piceatannol is a metabolic derivative of well-known anti-angiogenic compound resveratrol. Both (biochanin A and piceatannol) compounds were isolated from *Sophora interrupta*.[3] Biochanin A has shown to possess anticarcinogenic, anti-proliferative, and anti-inflammatory activity in different types of cancers such as the breast, pancreas, lung, and melanoma. Biochanin A has shown to possess chemopreventive efficiency against breast cancer[4] and to increase the tumor latency period, decreased the promotion of tumors, and decreased tumor multiplicity in rodents with chemically-induced mammary carcinogenesis.[5] It was found that biochanin A selectively targets human epidermal growth factor receptor 2-positive SK-BR-3 breast cancer cells without affecting normal breast epithelial cells (Michigan Cancer Foundation [MCF]-10A), and fibroblast cells (NIH-3T3).[6] Apart from breast cancer, this compound has also shown to play a potential role in the chemoprevention of prostate cancer through the enhancement of tumor necrosis factor-related inducing ligand-mediated apoptosis in LNCaP and DU145 prostate cancer cells,[7,8] shown to inhibit the activity of Protein Kinase-B (AKT) and MAPK pathways in pancreatic cancer cells, inhibition of nuclear factor-kappa B (NF-κB) and MAPK signaling pathway[9] in SK-Mel-28 melanoma cancer cell lines.

Piceatannol is a type of phenolic compound and belongs to the class of stilbenes.[10] Stilbenes (C6–C2–C6) are derived from the common phenylpropene (C6–C3) skeleton building block. Piceatannol has been found in various plants, including grapes, passion fruit, white tea, and Japanese knotweed.[11] Piceatannol is a metabolite of resveratrol and has shown to possess antitumor, antioxidant, and anti-inflammatory activities.[12] The key difference between resveratrol and piceatannol is the presence of an extra hydroxyl group at the C3 position of the aromatic rings.[13] Identical compound (s) were found in *Salvia yunnanensis*[14] and led to suppress the expression of vascular endothelial growth factors (VEGF) in the ECV304 cell line, it suggests that compounds from these family members possibly inhibit angiogenesis.[10] Piceatannol can inhibit cell proliferation by arresting the cell cycle in G0 and G1 phases in liver cancer cells and leukemic cells.[15] Piceatannol suppresses breast cancer cell invasion through the inhibition of Matrix metallopeptidase 9 (MMP-9); involvement of Phosphoinositide 3-kinase (P13K)/AKT, and nuclear factor kappa-light-chain-enhancer of activated B cells (NF-kB)[16]

Resveratrol is a dietary polyphenol with nutraceutical properties toward suppressing cancer cell growth in tumor microenvironment.[17] Resveratrol is a well-known anticancer compound with fewer side effects. Resveratrol has shown to suppress the proliferation of uterine cancer cells by inhibiting the WNT signaling pathway, breast cancer by inhibiting estrogen metabolism, pancreatic cancer by sensitizing DNA repair pathways, by upregulating cellular apoptotic missionary through PI3k/AKT signaling pathway, ovarian cancer cells by downregulation of Notch/PTEN/AKT signaling, gastric cancer cells by the inhibition of metastasis-associated lung adenocarcinoma transcript 1-mediated epithelial to mesenchymal transition (EMT).[18-22] EMT is the hallmark for cancer metastasis.[23] Metastatic cells have shown to undergo an altered metabolic pathway for procuring energy requirements for cell growth. Resveratrol has shown to alter the metabolic transformation by attenuating autophagy in cancer cells.[24]

MATERIALS AND METHODS

Cell viability and cell culture assay

Cells were cultured using established protocol.[25] In brief, 5×10^6 cells of MCF-7 cells were seeded in a 96 well plate and were maintained in Dulbecco's modified eagle's medium and F12K medium, respectively. Both the cell lines were supplemented with 10% fetal bovine serum (heat-inactivated) and 1% antibiotic (100 U/ml of penicillin and 100 µg/mL streptomycin) gently mixed and placed in a 5% CO_2-humidified incubator at 37°C. To study the anticancer activity of biochanin A, 5000 cells of breast (MCF-7) origin were seeded in a 96 well plate, cells were treated with increasing concentrations of biochanin A (1, 10, 50, 100, 250, 300, 500, and 1000 µg/ml) and dimethyl sulfoxide (DMSO) as a control for 24 h. Following incubation, 15 µl of 3 (4, 5 dimethyl thiazol 2yl) 2, 5 diphenyltetrazo- lium bromide (MTT) (5 mg/ml) reagent was added to the culture media and further incubated for 4 h at 37°C in CO_2 incubator. After an incubation period, MTT containing supernatant was aspirated, 200 µl of DMSO and 25 µl of Sorenson glycine buffer (0.1 M glycine and 0.1 M NaCl, pH 10.5) were added to lyse the cells and solubilize the water-insoluble formazan crystals. Absorbance values of the lysates were determined on a Fluostar Optima microplate reader (BMG Labtech, Germany) at 570 nm. The percentage of inhibition was calculated as:

$$\% \text{ cell viability} = \frac{\text{Mean OD of vehicle-treated cells} - \text{Mean OD of drug-treated cells}}{\text{Mean OD of vehicle-treated cells}} \times 100$$

The inhibitory concentration (IC_{50}) values were calculated using a GraphPad prism, version 5.02 software (GraphPad Software Inc., CA, U.S.A). Negative controls were maintained with DMSO. In a separate experiment, the effects of three extracts on cells were confirmed to observe the morphological changes such as cell shape. The size was captured using a phase contrast microscope (Zeiss, Axiovert 25, Germany).

Acridine orange/ethidium bromide staining

To validate the cellular permeability of the dyes, 0.5×10^6 cells of MCF-7 and PC-3 cells in a 6 well plate were seeded and cultured. Following 24 h of incubation, the media was replaced with fresh media consisting of biochanin-A and further allowed for incubation of 24 h at 37°C in a 5% CO_2 incubator. The cells were washed with phosphate buffer saline (PBS), added 100 µl of acridine orange (AO) and ethidium bromide (EtBr) (50 µg/ml each), respectively, to each well, and incubated for 15 min in CO_2 incubator. Following incubation, the medium was aspirated and washed thrice with PBS. The intensity of fluorescent staining was observed, and the images were captured with the help of a fluorescent microscope (Zeiss, Axiovert 25, Germany) using appropriate color filters.

In vitro scratch assay

To measure the cell proliferation/motility, performed *in vitro* scratch assay using MCF-7 cells. In brief, MCF-7 cells were seeded in a 6 well microtiter plate until about 90% confluent. The media was then removed, and equal size "scratch" was created using a pipette tip and then rinsed with PBS (phosphate buffered saline) to remove detached cells. The medium with the indicated concentrations of biochanin-A was then added for 24 h incubation in the presence of resveratrol as standard to control alteration in cell proliferation. The microscopic observations of the cells were recorded at 0, 6, 12, and 24 h after treatment. The images were captured using a fluorescent microscope (Zeiss, Axio-vert 25, Germany) under ×10 and analyzed using T-Scratch software v 7.8.

Fourier-transform infrared spectrometer

The data were collected and processed by analyst ChemStation software, and also Fourier-transform infrared (FT-IR) spectrometer equipped with (Lithium tantalite detector). The sample was introduced in Hygroscopic KBr glass windows were exactly 100 µL sample. FT-IR spectra were obtained by collecting 100 scans with spectra was collected

using a resolution of 64 cm^{-1}. A pure vehicle solvent was analyzed before each sample analysis as a background. The FT-IR spectrum corrected and baseline ranging in 4000–450 cm^{-1} was recorded using Spectrum™ two spectroscopy software (PerkinElmer Corporation, Lambda).

Molecular docking and dynamic (MD) simulations

GLIDE module version 6.1 in the Schrödinger suite, a grid-based ligand docking method with energetics, was used for ligand docking. A grid box with the size 72 × 72 × 72 Å with coordinates X = 12.188, Y = 20.152, and Z = 48.922 were generated at the centroid of the crystal ligand as the grid-based protocol requires a grid for ligand docking. Using the Extra-precision (XP) mode in the ligand docking protocol, the prepared metabolites (ligands) were docked into the active pockets of VEGF receptor 1 (VEGFR1) and R2. Based on the G-scores, the ligands were ranked and the interactions between amino acids of protein and ligand were analyzed. The interactions were depicted using ligplots.

All the simulations performed with the Desmond version 2013 to study the stability of the protein-ligand complex. In the present study, prepared protein-ligand complex was subjected to the TIP4P water model in an orthorhombic periodic boundary box of size 376,702 Å for 3HNG complexes and 440,055 Å for 3U6J complexes under a solvated condition using the system builder. To neutralize the system, three Cl^- ions are added based on the total charge of the system, and also a salt concentration of 0.15 M was added to maintain the charge of the complex. After building the prepared model system, the total number of atoms present in the built system was calculated, and the system was minimized up to a maximum of 5000 iterations. Further, MD simulations, studies were carried out with a periodic boundary condition in the isothermal–isobaric ensemble (NPT) ensemble, the temperature at 300 K, 1 atmospheric pressure and the model was relaxed using default relaxation protocol integrated with the Desmond. The simulation job was carried out to all the VEGFR1 and R2 complexes along with standard over a time period of 10 nanoseconds (ns) with 5 ns intervals, the time step of 5 ns. The final trajectory file was taken for calculating the root-mean-square deviation (RMSD), root-mean-square fluctuation, and total energy of the complexes.

Anti-angiogenesis activity using the chorioallantoic membrane

The ability of biochanin-A to inhibit angiogenesis was determined using a modified chorioallantoic membrane (CAM) assay described by.[26] The fertilized eggs on day-1 were purchased from the local vendors and shell surface disinfected using 70% ethanol and transferred to an incubator (GENEI, Bengaluru, Karnataka, India) at 37°C with 75% humidity for optimal growth conditions. For equal distribution of the blood vessels, the eggs are turned over twice in a day. On day-8, the eggs were again disinfected with ethanol (70%), and a square-shaped window of 1 cm^2 was opened in the eggshell with a saw blade exposing the white inner shell membrane. Biochanin A was dissolved in (DMSO) at variable concentrations and applied to the sterile Whatman membrane sheet. The extract was air-dried on the disinfected environment and implanted on the outer third of growing CAM blood vessels. Controls were treated with blank DMSO discs. The distinct allantoic blood vessels around the DMSO discs were examined 15 and 30 min after implantation. The angiogenic responses were captured using a high resolution (NIKON) Camera. The images were imported into the AngioQuant software to score the number of sizes and the length of the blood vessels. Black and white skeleton prune images are generated corresponding to the correct color images. The intensity of individual vessel was quantified by densitometry using AngioQuant software. Values were represented in total length and its size of tubules as well as mean length and its size of tubules corresponding to the kernel size 1, a segment not to remove edge tubules, prune size to be 10 according to AngioQuant software, Tampere University of Technology, Finland.

Statistical analysis

Data were analyzed using GraphPad Prism® 5 (Version 5.01, GraphPad software, Inc., San Diego, CA, USA). Results are expressed as the mean ± Standard deviation of three independent experiments. The data were analyzed for statistical significance by one-way ANOVA test; $P < 0.05$ was considered to be statistically significant.

RESULTS

Anticancer activity of compounds on Michigan cancer foundation-7 cells

To identify anticancer activity, MCF 7 cells were treated with increasing concentration of piceatannol, biochanin-A, and resveratrol (50, 100, 250, 500, and 1000 µg/ml). Following incubation, cell viability was measured using MTT assay. Results showed that the compounds have no impact on cell viability until the concentration of 50 µM and above the cell growth gradually declined and reached to the maximum concentration of 500 µM. The half-maximal IC_{50} for resveratrol and piceatannol is found to be 250 µM, and for biochanin-A is 150 µM [Figure 1a]. Based on the MTT assay, in a separate experiment, the cells were treated with all three compounds at a concentration equivalent to IC_{50} values, (250 µM and 150 µM) and measured the apoptotic index using AO and EtBr dye dyes. The use of AO/EB staining demonstrated that the live and dead cells. As shown in Figure 1b, cells treated with compounds showed both bright red fluorescent (dead) and green fluorescent (live) as compared to control treated cells indicating cell death. Merged images indicate the co-localization of green and red (orange) color indicates cells undergoing apoptosis, which is more prominent in treated cells as compared to untreated cells. To test the action of compounds on cancer cell migration and proliferation, we performed a standard *in vitro* scratch/wound assay. As shown in Figure 1c, drug-treated cells were unable to migrate from the cleared area until 24 h of incubation. On the other hand, vehicle-treated cells filled the gap with newly dividing cells, which is evident from the distance between the cleared regions from 0 h to 24 h. Next, we calculated the percentage inhibition of cell proliferation using T-Scratch Software (http://www.cse-lab.ethz.ch). As shown in Figure 1d, the vehicle-treated cells had filled in the cleared area by about 58% while piceatannol (24%), biochanin-A (45%), and resveratrol (35%) of cell migration. Thus, the migration of cancer cells was significantly reduced in both piceatannol and biochanin-A treated plates and interestingly, it was significantly more prominent. These results, therefore, indicate that piceatannol and biochanin-A effectively lowered the proliferation of breast cancer cells.

Fourier-transform infrared spectra to evaluate the metabolic changes induced by biochanin-a, piceatannol, and resveratrol on breast cancer cells

To test the compound efficacy against the anticancer activity, we treated MCF-7 cells with piceatannol, resveratrol, and biochanin-A at a concentration equivalent to IC50 values, (250 µM and 150 µM). Following 24 h, culture media was separated from the cells by centrifugation. Metabolic changes of the compounds were confirmed by FT-IR analysis. The FT-IR spectra showed several characteristic absorptions peaks and variable stretching and bending for compound alone, media with compound, and compound treated cells. As shown in Figure 2a (lower panel), piceatannol alone has characteristic

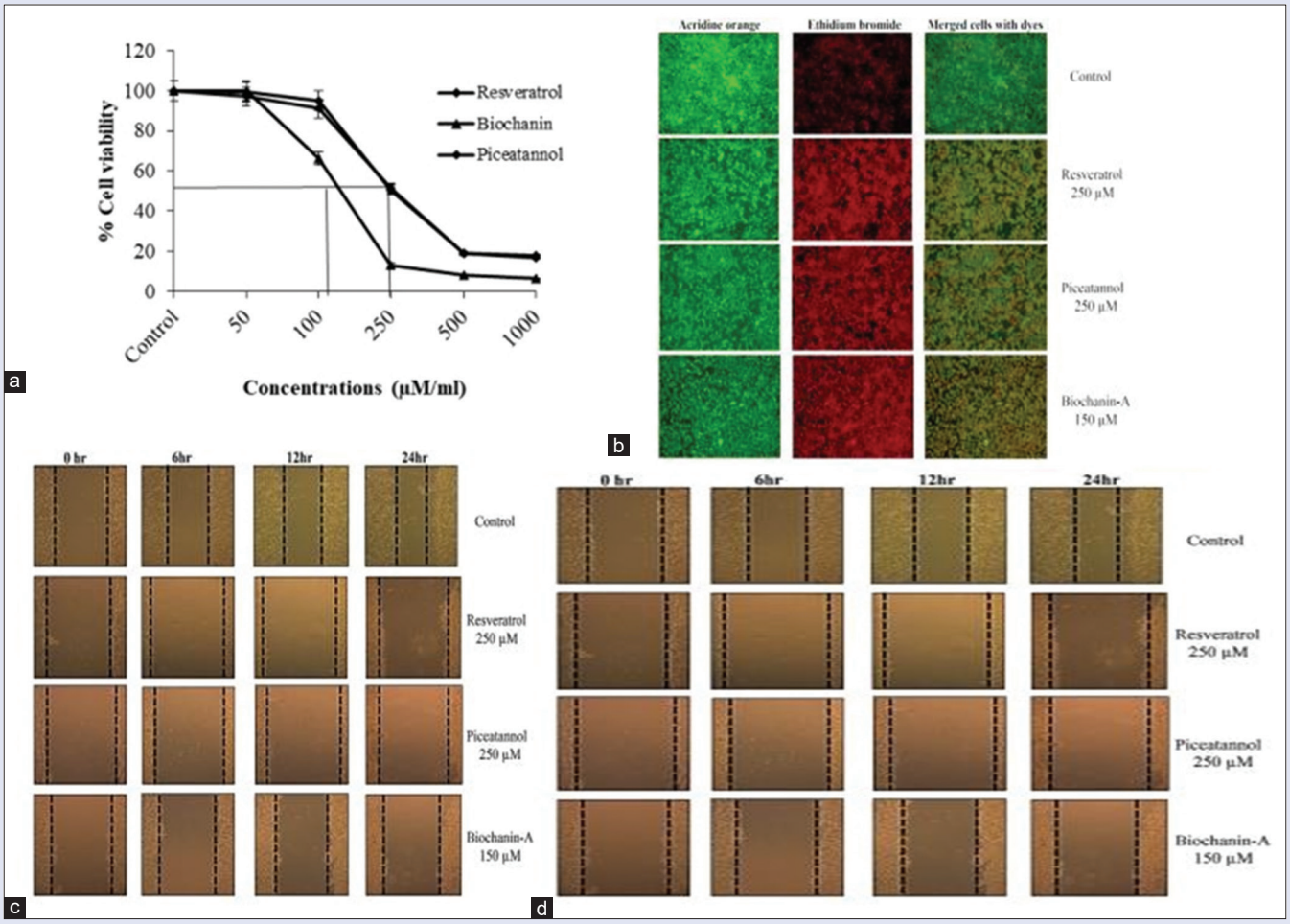

Figure 1: Cell viability and motility assay. (a) Cytotoxicity curves of resveratrol, biochanin-A, and piceatannol on Michigan Cancer Foundation-7 cell line by 3 (4, 5 dimethyl thiazol 2yl) 2, 5 diphenyltetrazo- lium bromide assay. (b) Apoptotic assay on Michigan Cancer Foundation-7 cells with acridine orange/ethidium bromide dyes. The orange- and red-color pattern indicates cell viability. (c) Wound healing assay on Michigan Cancer Foundation-7 cells in the presence and absence of compounds (×20). (d) Graph depicting the percentage of migration at 0, 12, and 24 h. The data are representative of three independent experiment groups and significance indicated as mean ± standard deviations

absorption peaks in the range 3000–3500 cm^{-1}, and 1650 cm^{-1}, which was attributed to the phenolic hydroxyl group and stretching vibration of -C=C- of the aromatic ring of piceatannol supported by = CH alkenes and aromatics (683 and 794 cm^{-1}), respectively. Whereas, few of the functional groups appeared in piceatannol treated cells, at 3386 and 3206 cm^{-1}, which was attributed to O–H stretch of a phenolic group in treated cells Figure 2a (Upper panel). As shown in Figure 2b, the FT-IR spectrum of resveratrol is moreover like piceatannol in the range of 450–3000 cm^{-1} Figure 2b (lower panel). However, new peaks had appeared in the range of 3000–3500 cm^{-1} (Upper panel). It suggests that the phenolic hydroxyl group has undergone certain unknown structural changes between piceatannol and resveratrol following treatment with cells. On the other hand, Biochanin-A Figure 2c, spectra showed a characteristic C=O functional group at 1653 cm^{-1}. The broadband at 3632 cm^{-1} and a medium band around 1166 cm^{-1} was assigned to hydrogen-bond stretching and C-O-C linkage, respectively (Lower panel). In compound treated samples the absorption peaks displayed downward shifts 3632 cm^{-1}-3443 cm^{-1}; 3334 cm^{-1}-3292 cm^{-1} and 2981 cm^{-1}-2977 cm^{-1} across the spectrum ranging from 4000 to 2500 cm^{-1}. The features around 1000–2000 cm^{-1} of the biochanin-A spectrum infer stretching vibrations of the benzene ring (upper panel). Taken together, this data suggests that all three compounds were undergone dynamic structural changes and no similar peaks were identified between free compounds versus treated cells. It suggests that the free form of the compound is no more available in the media for further utilization of cells.

Identification of active site amino-acid contacts with biochanin-a, piceatannol, and resveratrol in vascular endothelial growth factor receptors

VEGFs R1 and R2 were both subjected to XP docking with biochanin-A, piceatannol, and resveratrol. Glide scores and hydrogen-bond interactions were obtained for biochanin-A piceatannol, and resveratrol [Table 1]. As shown in Figure 3a and d, Piceatannol was found deep into the narrow pocket formed by the inner lobe cleft as reported in the X-ray crystallographic structures. Piceatannol had strong hydrogen bond interactions with VEGFR1 (3HNG) in various amino acids Cys912 (two hydrogen bonds), Glu878, Lys861 (π-cation), and Phe1041 (π- π stacking), with a glide score of – 10.193. Piceatannol inside the active site of VEGFR2 (3U6J) was maintained with the help of single hydrogen bond at Cys919, Asp1046, and Lys868 (π-cation), with a glide score of –8.359. As shown in Figure 3b and e, resveratrol inside the active site of VEGFR1 engaged in single hydrogen bond interactions

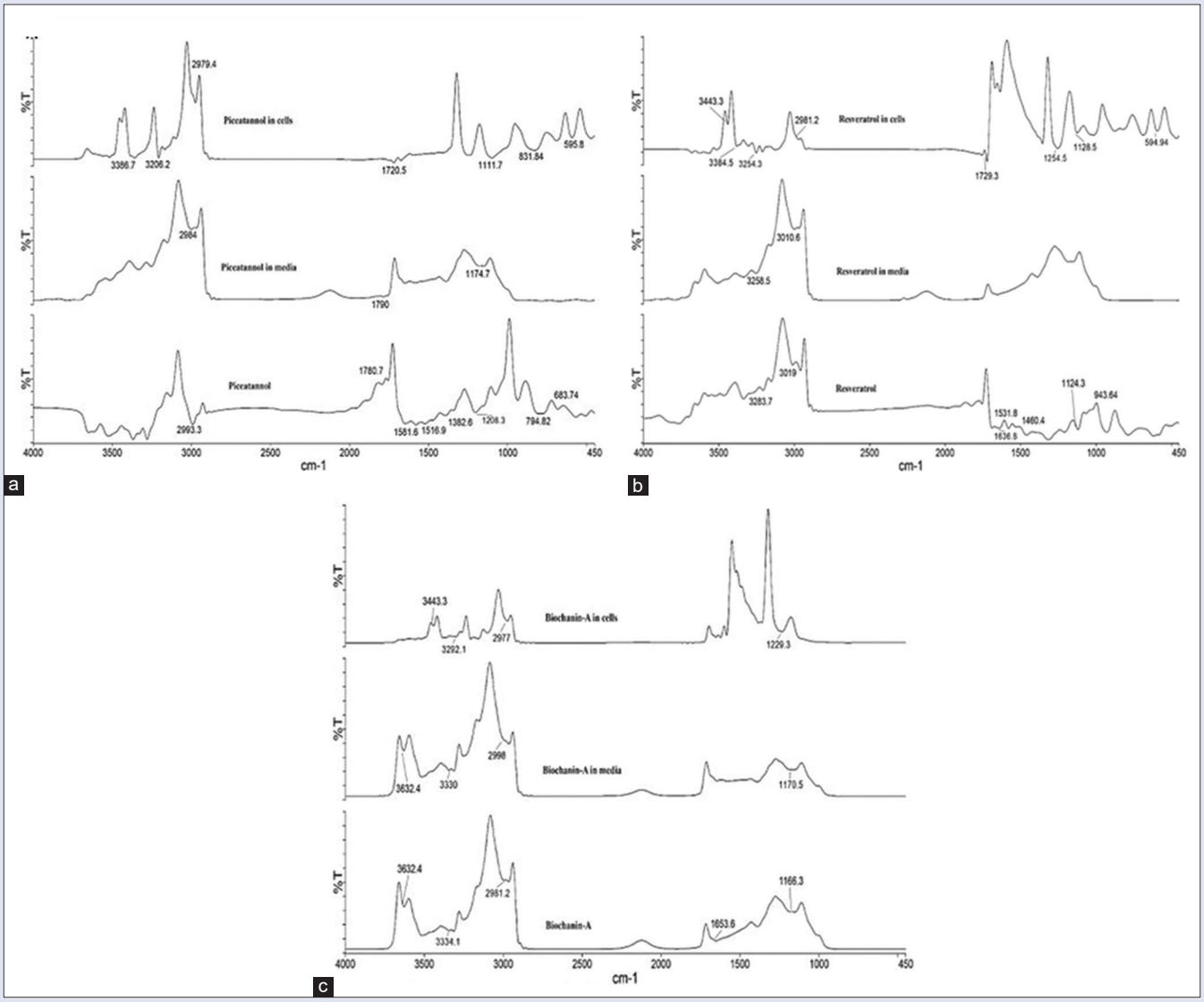

Figure 2: Metabolic changes of compound determination by Fourier-transform infrared analysis. (a) Piceatannol. (b) Resveratrol. (c) Biochanin-A

Table 1: Glide scores with predicted interactions of piceatannol, resveratrol, and biochanin-A to vascular endothelial growth factor R1and vascular endothelial growth factor R2

Ligand	Proteins	Glide score	Amino acid interactions
Piceatannol	VEGFR1	−EGF	Cys912, Lys861, (π-cation)
	VEGFR2	−EGFR	Cys919 (2H), Asp1046
Resveratrol	VEGFR1	−EGFR1	Cys912, Glu878, Lys861 (π-cation)
	VEGFR2	−EGFR2	Lys868, Asp1046, Cys914
Biochanin-A	VEGFR1	−EGF	Cys912, Lys861(π -cation)
	VEGFR2	−EGFR	Cys919 (2H), Asp1046

VEGF: Vascular endothelial growth factor

with Cys912 and Asp1040, with a glide score of -8.787 and resveratrol-VEGFR2 docking interactions showed Cys919 (two hydrogen bonds) and Lys868, with a glide score of -8.226 respectively. As shown in Figure 3c, Biochanin-A was found deep into the narrow pocket formed by the inner lobe cleft as reported in the X-ray crystallographic structures. Biochanin-A had strong hydrogen bond interactions with VEGFR1 (3HNG) in various amino acids Cys912 (two hydrogen bonds), Glu910 (H-bond), and Phe1041 (π- π stacking), with a glide score of −10.077. As shown in Figure 3f, Biochanin-A inside the active site of VEGFR2 (3U6J) was maintained with the help of two hydrogen bonds at Cys919, Glu917, and Thr916 (H-bond side chain), with a glide score of −8.932.

Molecular dynamics simulations of biochanin-A, piceatannol, and resveratrol with vascular endothelial growth factors R1 and vascular endothelial growth factors R2

The ligand-protein complexes were subsequently subjected to molecular dynamics (MD) simulations using the Desmond module. Accordingly, a 10 ns simulation run was conducted across the compounds and hydrogen bond interactions of receptor and ligand complexes before and after simulations are reported in Table 2. Deviations in VEGFR1 protein for piceatannol, resveratrol, and biochanin-A started initially at 0.6 Å, 0.75Å, and 1.0 Å, and sustained their stability from until 10 ns for all the compounds tested. However, in the case of piceatannol, there is a sudden deviation in the ligand between 8.2 and 9 ns (frames 1785–1818),

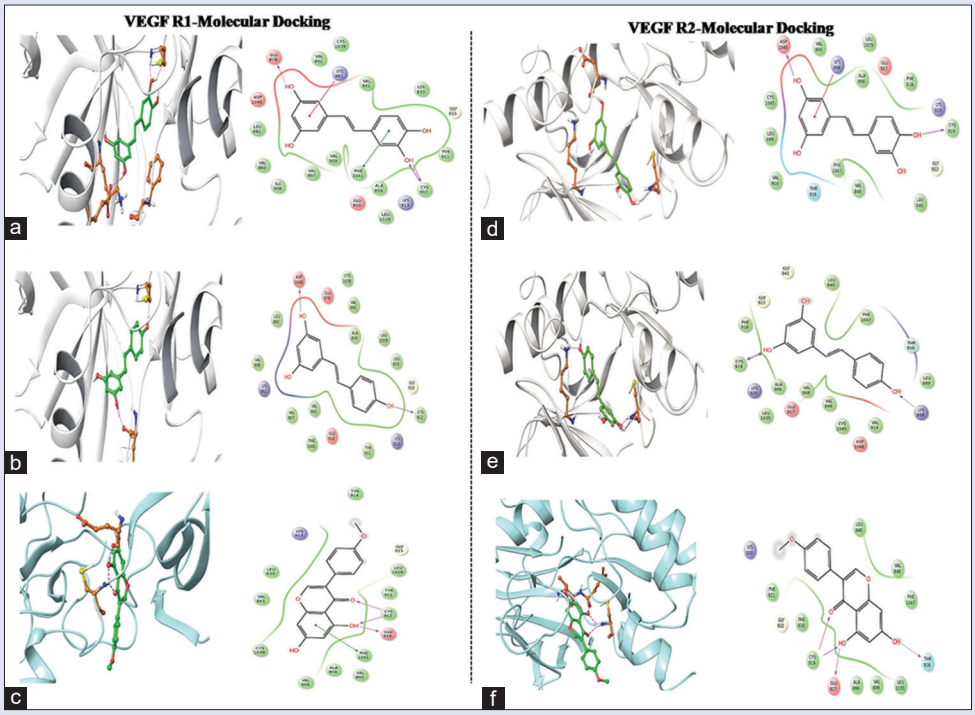

Figure 3: Molecular docking studies. Three dimensional and *in silico* two dimensional plots of 3HNG and 3U6J (vascular endothelial growth factors receptor 1 and vascular endothelial growth factors receptor 2) interaction with (a and d) Piceatannol (b and e) resveratrol (c and f) biochanin-A. Violet-color arrows indicate hydrogen-bond interaction with receptors

Table 2: The Percentage of hydrogen bond interaction between active amino acid residues of protein and ligands

		Aminoacids interactions		H-Bond formation	
Proteins	**Ligands**	**Before MD**	**After MD**	**Before MD**	**After MD**
VEGFR1	Resveratrol	Cys912, Glu878, Lys861 (π-cation)	Glu878, Ala 859, Asp 1040, Val 907	2	4
	Piceatannol	Cys912, Glu 878, Lys861 (π-cation)	Cys912, Ala 859, Glu878	2	3
	Biochanin-A	Cys912, Glu 910	Glu910, Cys 912, Tyr911 (π-π cation)	2	2
VEGFR2	Resveratrol	Lys868, Cys919	Cys919, Thr 916, Phe1047 (π-π cation)	2	2
	Piceatannol	Cys919, Asp1046	Glu 917, Thr 916, Phe1047 (π-π cation), Phe918 (π-π cation)	2	2
	Biochanin-A	Cys919 (2H), Glu917, Thr916	Glu 917, Cys 919, Phe1047 (π-π cation), Phe918(π-π cation)	2	2

VEGF: Vascular endothelial growth factor; MD: Molecular docking and dynamic

which was observed as a comparison to resveratrol during the simulation event analysis. However, the total RMSD does not deviate above 2.7 Å indicating the stability of the complex. On the other hand, the deviations of biochanin-A started initially and showed 2.8 Å elevation immediately and came down to 1.2 Å at 1 ns and maintained its stability up to 6 ns without any deviations. Then again elevated to 2.4 Å and maintained stability up to 10 ns without any deviations. Despite deviations, we found that this compound sustained its stability from 6.1 ns until 10 ns with an RMSD between 0.5 Å and 2.8 Å. It has not shown any difference in ligand confirmation except changes in the deviations of the loops present in the protein. Deviations in VEGFR2 protein for piceatannol, resveratrol, and biochanin-A started initially at 0.8Å, 0.8Å, and 0.75Å, respectively. In the case of piceatannol, stable deviations were observed between 1 ns and 9.5 ns interval at 3.2 Å and can observe a minor deviation until 10 ns up to 4.2 Å. In the case of resveratrol, the deviations started initially, and stability is found until 1.8 ns, and an immediate increase in the deviation from 2.0 Å to 3.5 Å was observed, which is further continued up to 10 ns [Figure 4]. Unlike piceatannol, resveratrol, VEGFR2 deviations with biochanin-A were maintained in the range between 0.75 Å and 2.0 Å and obtained stability after 1 ns and sustained till the last frame.

Chorioallantoic membrane assay

To determine the structure-function relationship, we have performed *in ovo* CAM assay. In brief, a square-shaped window of 1 cm^2 was opened in the eggshell with a saw blade exposing the white inner shell membrane. All three compounds were dissolved in 0.1% DMSO in PBS at variable concentrations (250, 500, and 750 μM/ml). Circle shape discs were dipped in respective concentrations and placed on growing blood vessels. Controls were treated with blank DMSO discs. Following 6 h, the images were captured [Figure 5] and the length and size of the blood vessels density were recorded using AngioQuant software. The length and size of the blood vessels were calculated as a fold change. As depicted in Figure 5a and b, the length and size of the blood vessels decreased in a dose and time-dependent manner. The anti-angiogenic potential of piceatannol is proportional to resveratrol as well as biochanin A. Overall, it suggests that both the compounds inhibit sprouting of a new blood vessel from the chicken aorta and microvessels.

DISCUSSION

Biochanin-A possesses many bioactivities such as inhibitory and apoptogenic activities on cancer cells as well as anti-inflammatory

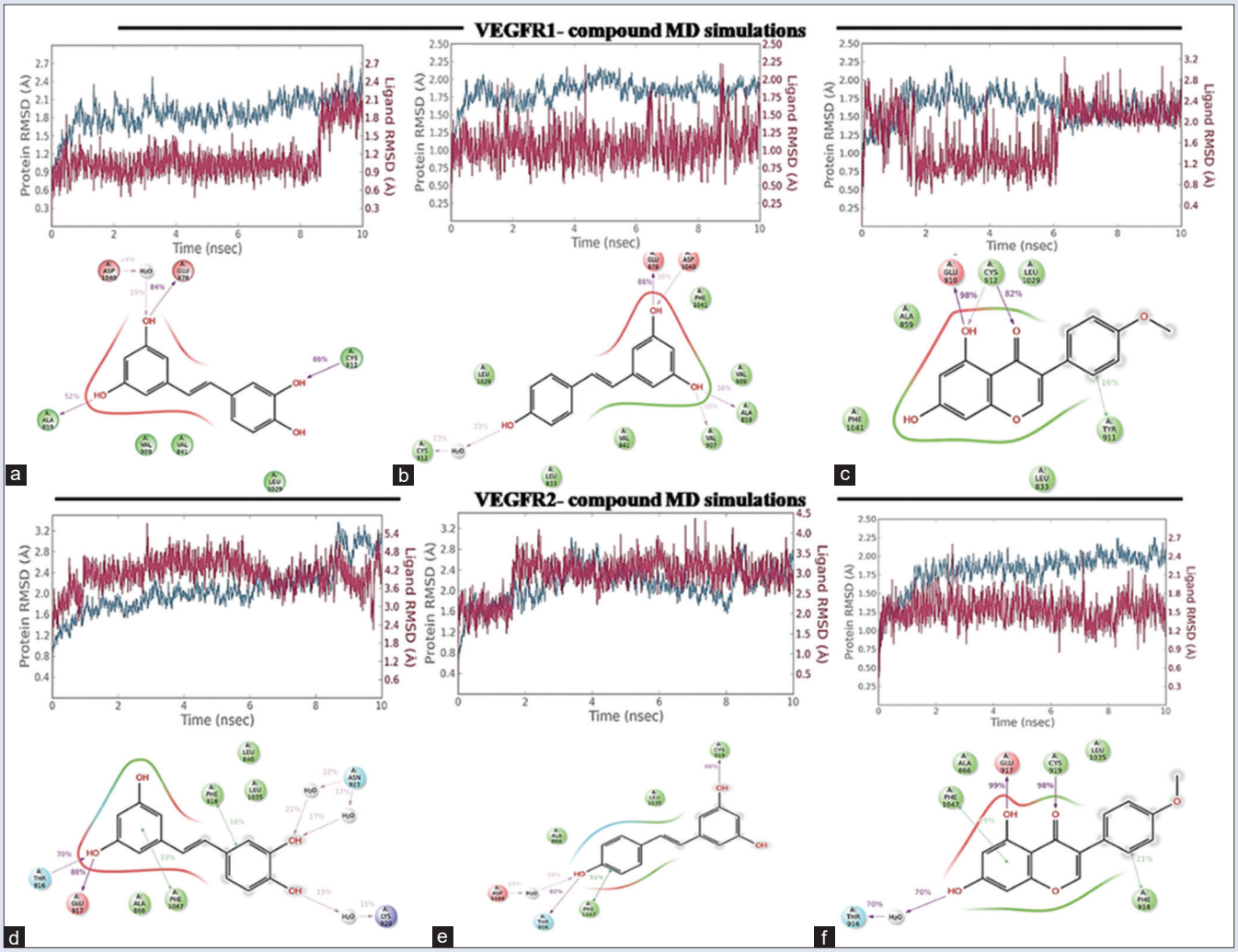

Figure 4: Molecular dynamic simulations trajectory depicting the root-mean-square deviation of vascular endothelial growth factors receptor 1 and vascular endothelial growth factors receptor 2 protein and ligand interactions with (a and d) Piceatannol (b and e) Resveratrol (c and f) Biochanin-A

and anti-proliferative activities in RAW 264.7 cells by blocking NF-κB activation. Interestingly, biochanin-A also has shown antiangiogenic effects on murine brain endothelial (b End. 3) cells.[27] Sprouting new blood vessels from preceding capillaries and post-capillary venules is called angiogenesis.[28] Angiogenesis in several physiological and pathological circumstances, such as during embryonic development and wound healing, as well as in patients with chronic inflammatory diseases and various metastatic tumor growths.[29] To study the anticancer activities of biochanin A, performed *in vitro* scratch assay. *In vitro* scratch experiment is widely recognized for determining the proliferation rate of cancer cells in the presence and absence of anticancer compounds.[30] In the scratch assay analysis, piceatannol and biochanin-A inhibited the 76% and 55% of cancer cell proliferation of MCF-7 cells and resveratrol also inhibited 65% cell proliferation. It indicates that the anticancer secondary metabolites were unable to fill the open area of the scratch, indicating the antiproliferation activity and another experiment for determining the apoptosis by AO/EtBr also shown cell death. Overall, it suggests that the compounds have shown anticancer activities. Bioavailability of the compounds was confirmed by FT-IR analysis.[31] The FT-IR spectra showed several characteristic absorptions peaks and variable stretching and bending for compound alone, media with compounds, and compound treated cells. Indeed, this data suggest that all the three compounds were undergone dynamic structural changes, and no similar peaks were identified between free drugs versus treated cells.[32] It suggests that the free form of the compound is no more available in the media for further utilization of cells. To validate, the anti-angiogenic activity of piceatannol, a metabolic product of resveratrol and biochanin-A were docked to VEGFR1 and R2. Based on the literature, the important amino acids responsible for binding activity in the binding pocket were Lys861, Glu878, Asp1040, and Cys912 for VEGFR1 and Cys919, Phe1047, Lys868, and Asp1046 for VEGFR2. The molecular docking study shows that both resveratrol and piceatannol has shown interactions with Cys912, Glu878, Lys861 (π-cation) of VEGFR1, and Cys919 with VEGFR2.

Piceatannol has shared common interactions with VEGFR1 and R2 proteins. In a similar way, piceatannol has shown additional interaction (Asp1046) with VEGFR2 compared with resveratrol (Lys868). This may be due to the presence of an extra hydroxyl group in piceatannol, it has shown a high docking score as compared with resveratrol. This is because the hydroxyl group is in good orientation with the acidic part of the binding pocket which is absent in resveratrol. Biochanin-A has shown common interactions with Cys912 of VEGFR1 in compare to resveratrol and Cys919 (2H), Glu917, and Thr916 interactions with VEGFR2

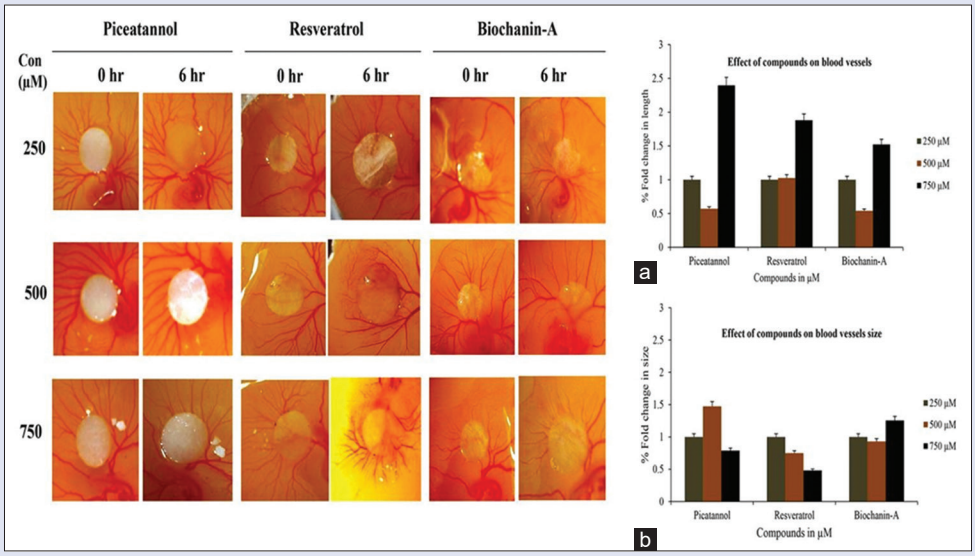

Figure 5: Effects of compounds on chorioallantoic membrane. Images of chorioallantoic membrane treated with 250, 500, and 750 μM. Chorioallantoic membrane treated with dose and time (0–6 h) dependent manner shows a decrease in vascularization. (a) The graph depicts the length of the blood vessel and (b) the size of the blood vessel

proteins. All three compounds have shown similar orientation in the binding pocket. The MD simulations were performed to examine the stability of compounds in conjunction with VEGF receptors. Piceatannol-VEGFR1 complex displayed new hydrogen-bond interaction (Glu878) during the stipulated period of MD simulations. Biochanin-A-VEGFR1 complex displayed an extra bond interaction, i.e.,; (Tyr911) π-π cation during the period of MD simulations. In docking analysis, piceatannol formed hydrogen bond interactions with Glu912, Glu878, and biochanin-A formed hydrogen-bond interactions with Cys912, Glu910 amino acids. VEGFR1-resveratrol complex displayed completely new hydrogen-bond interactions after MD simulations as compared to docking poses. However, the interactions of the compounds with VEGFR1 were minimal before and after MD simulations. It suggests that the resveratrol has varied its orientation leading to less stable compound as compared to the piceatannol and biochanin-A. In VEGFR2-piceatannol complex showed a different type of interactions before and after MD simulations, i. e, Glu917, Thr916, Phe1047 (π-π cation), and Phe918 (π-π cation) are new interactions after MD simulations. Interaction profile of VEGFR2-Resveratrol complex showed H-bond with Cys919 which was observed before and after simulations and Lys868 which formed before MD simulations and Thr916, Phe1047 (π-π cation) formed only after MD simulations. The interactions of the VEGFR2-Biochanin-A before MD simulations were Glu917, Cys919, and Thr916 and after MD simulations Glu917, Cys919, Phe1047 (π-π cation), Phe918 (π-π cation). Glu917, Cys919 was sustained throughout the simulation making it a stable molecule when compared to resveratrol. After MD simulations, VEGFR2-resveratrol complex reported Cys919 as common interactions in comparison to before MD simulations; this is because of the low levels of change in binding patterns. However, the interactions of the compounds with VEGFR2 were almost similar to the important amino acids before and after MD simulations. This was due to the stable conformation and orientation of the compounds. From this, it can be concluded that the piceatannol and biochanin-A were equally potent when compared to resveratrol. Furthermore, this is supported by *in ovo* CAM model which acts an angiogenic model with sprouting blood vessels. The compounds expressed their suppression of length and size of blood vessels which conveys the disruption of actin stress fibers and focal adhesions in endothelial cells is an established mechanism contributing to endothelial cell disassembly, which is a possible event involved in anti-angiogenesis.[33]

CONCLUSION

Overall, our results indicate that the biochanin A, a naturally extract compound can deregulate many of the cancer properties such as cell viability and cell motility and also anti-angiogenic properties by interacting with two of the VEGFs R1 and R2. Moreover, our results are in accordance with well-known anticancer compounds piceatannol and resveratrol.

Acknowledgement

The authors would like to thank the Koneru Lakshmaiah Education Foundation of KL (Deemed to be) University.

Financial support and sponsorship

Nil.

Conflicts of interest

There are no conflicts of interest.

REFERENCES

1. Hanski L, Genina N, Uvell H, Malinovskaja K, Gylfe Å, Laaksonen T, *et al.* Inhibitory activity of the isoflavone biochanin A on intracellular bacteria of genus *chlamydia* and initial development of a buccal formulation. PLoS One 2014;9:e115115.
2. Spagnuolo C, Russo GL, Orhan IE, Habtemariam S, Daglia M, Sureda A, *et al.* Genistein and cancer: Current status, challenges, and future directions. Adv Nutr 2015;6:408-19.
3. Mathi P, Nikhil K, Das S, Roy P, Bokka VR, Botlagunta M. Evaluation of *in vitro* anticancer activity and GC-MS analysis from leaf *Sophora interrupta* Bedd. Int J Pharm Pharm Sci 2015;7.303-8.
4. Colditz GA, Wolin KY, Gehlert S. Applying what we know to accelerate cancer prevention. Sci Transl Med 2012;4:127rv4.
5. Gupta RC. Nutraceuticals: Efficacy, Safety and Toxicity. Academic Press; 2016.
6. Sehdev V, Lai JC, Bhushan A. Biochanin A modulates cell viability, invasion, and growth promoting signaling pathways in HER-2-positive breast cancer cells. J Oncol

2009;2009:121458.

7. Szliszka E, Czuba ZP, Mertas A, Paradysz A, Krol W. The dietary isoflavone biochanin-A sensitizes prostate cancer cells to TRAIL-induced apoptosis. Urol Oncol 2013;31:331-42.
8. Watson RR. Foods and Dietary Supplements in the Prevention and Treatment of Disease in Older Adults. Academic Press; 2015.
9. Xiao P, Zheng B, Sun J, Yang J. Biochanin A induces anticancer effects in SK-Mel-28 human malignant melanoma cells via induction of apoptosis, inhibition of cell invasion and modulation of NF-κB and MAPK signaling pathways. Oncol Lett 2017;14:5989-93.
10. Kim A, Ma JY. Piceatannol-3-O-β-D-glucopyranoside (PG) exhibits *in vitro* anti-metastatic and anti-angiogenic activities in HT1080 malignant fibrosarcoma cells. Phytomedicine 2019;57:95-104.
11. Seyed MA, Jantan I, Bukhari SN, Vijayaraghavan K. A comprehensive review on the chemotherapeutic potential of piceatannol for cancer treatment, with mechanistic insights. J Agric Food Chem 2016;64:725-37.
12. Dias SJ, Li K, Rimando AM, Dhar S, Mizuno CS, Penman AD, *et al.* Trimethoxy-resveratrol and piceatannol administered orally suppress and inhibit tumor formation and growth in prostate cancer xenografts. Prostate 2013;73:1135-46.
13. Androutsopoulos VP, Papakyriakou A, Vourloumis D, Tsatsakis AM, Spandidos DA. Dietary flavonoids in cancer therapy and prevention: Substrates and inhibitors of cytochrome P450 CYP1 enzymes. Pharmacol Ther 2010;126:9-20.
14. Daikonya A, Kitanaka S. Polyphenols from *Sophora yunnanensis*, and their inhibitory effects on nitric oxide production. Chem Pharm Bull (Tokyo) 2011;59:1567-9.
15. Ahmad Tajudin Tuan Johari S, Hashim F, Iryani Wan Ismail W, Manaf Ali A. A review on biological activities of Gelam honey. Journal of Applied Biology and Biotechnolog 2019;7:71-8.
16. Shrestha A, Pandey RP, Sohng JK. Biosynthesis of resveratrol and piceatannol in engineered microbial strains: Achievements and perspectives. Appl Microbiol Biotechnol 2019;103:2959-72.
17. Han Y, Jo H, Cho JH, Dhanasekaran DN, Song YS. Resveratrol as a tumor-suppressive nutraceutical modulating tumor microenvironment and malignant behaviors of cancer. Int J Mol Sci 2019;20. pii: E925.
18. Jiang Y, Xie Z, Yu J, Fu L. Resveratrol inhibits IL-1β-mediated nucleus pulposus cell apoptosis through regulating the PI3K/Akt pathway. Biosci Rep 2019;39. pii: BSR20190043.
19. Poschner S, Maier-Salamon A, Thalhammer T, Jäger W. Resveratrol and other dietary polyphenols are inhibitors of estrogen metabolism in human breast cancer cells. J Steroid Biochem Mol Biol 2019;190:11-8.
20. Yang Z, Xie Q, Chen Z, Ni H, Xia L, Zhao Q, *et al.* Resveratrol suppresses the invasion and migration of human gastric cancer cells via inhibition of MALAT1-mediated epithelial-to-mesenchymal transition. Exp Ther Med 2019;17:1569-78.
21. Vendrely V, Amintas S, Noel C, Moranvillier I, Lamrissi I, Rousseau B, *et al.* Combination treatment of resveratrol and capsaicin radiosensitizes pancreatic tumor cells by unbalancing DNA repair response to radiotherapy towards cell death. Cancer Lett 2019;451:1-0.
22. Mineda A, Nishimura M, Kagawa T, Takiguchi E, Kawakita T, Abe A, *et al.* Resveratrol suppresses proliferation and induces apoptosis of uterine sarcoma cells by inhibiting the Wnt signaling pathway. Exp Ther Med 2019;17:2242-6.
23. Xie M, Vesuna F, Botlagunta M, Bol GM, Irving A, Bergman Y, *et al.* NZ51, a ring-expanded nucleoside analog, inhibits motility and viability of breast cancer cells by targeting the RNA helicase DDX3. Oncotarget 2015;6:29901-13.
24. Deng S, Shanmugam MK, Kumar AP, Yap CT, Sethi G, Bishayee A. Targeting autophagy using natural compounds for cancer prevention and therapy. Cancer 2019;125:1228-46.
25. Bheemanapally K, Thimmaraju MK, Kasagoni S, Thatikonda P, Akula S, Kakarla L, Gummadi SB, Nemani H, Botlagunta M. *In vitro* anti-cancer activity of rosuvastatin and ketorolac nanoformulations against DDX3. J Young Pharm, 9(4), 2017, p.537.
26. Moreno-Jiménez I, Hulsart-Billstrom G, Lanham SA, Janeczek AA, Kontouli N, Kanczler JM, *et al.* The chorioallantoic membrane (CAM) assay for the study of human bone regeneration: A refinement animal model for tissue engineering. Sci Rep 2016;6:32168.
27. Jain A, Lai JC, Bhushan A. Biochanin A inhibits endothelial cell functions and proangiogenic pathways: Implications in glioma therapy. Anticancer Drugs 2015;26:323-30.
28. Ribatti D, Crivellato E. "Sprouting angiogenesis", a reappraisal. Dev Biol 2012;372:157-65.
29. Ono M. Molecular links between tumor angiogenesis and inflammation: Inflammatory stimuli of macrophages and cancer cells as targets for therapeutic strategy. Cancer Sci 2008;99:1501-6.
30. Ingrassia L, Lefranc F, Dewelle J, Pottier L, Mathieu V, Spiegl-Kreinecker S, *et al.* Structure-activity relationship analysis of novel derivatives of narciclasine (an *Amaryllidaceae* isocarbostyril derivative) as potential anticancer agents. J Med Chem 2009;52:1100-14.
31. Wu BB, Gong YP, Wu XH, Chen YY, Chen FF, Jin LT, *et al.* Fourier transform infrared spectroscopy for the distinction of MCF-7 cells treated with different concentrations of 5-fluorouracil. J Transl Med 2015;13:108.
32. Cakmak G, Zorlu F, Severcan M, Severcan F. Screening of protective effect of amifostine on radiation-induced structural and functional variations in rat liver microsomal membranes by FT-IR spectroscopy. Anal Chem 2011;83:2438-44.
33. Nagaraju GP, Sharma D. Anti-cancer role of SPARC, an inhibitor of adipogenesis. Cancer Treat Rev 2011;37:559-66.